Disturbances in the Wavenumber-Frequency Domain Observed Along 50° N*

Horst Böttger[1]) and Klaus Fraedrich

Institut für Meteorologie
Freie Universität Berlin
D–1000 Berlin, Fed. Rep. of Germany

(Manuscript received 12.7.1979, in revised form 6.11.1979)

Abstract:

For summer 1969 and winter 1969/70 spectral analysis of geopotential, mean temperature of thickness layers and meridional geostrophic wind along 50° N on selected tropospheric and stratospheric pressure levels is carried out 1. to establish climatic statistics for winter and summer which describe the known macro-turbulent processes of the planetary circulation in the westwind zones and 2. to obtain a statistical description in space and time of the structure of zonally and time averaged mid-latitude disturbances of the Northern Hemisphere. For the 500 mb level these analyses are extended to ten winters (1969/70–78/79) and five summers (1969, 1975–78) to estimate the year-to-year variability.

When averaged with respect to longitude and time, the variable $q(\lambda, t)$ – where q is geopotential, temperature, or meridional geostrophic wind – is given by four terms: the time and zonal average, the fluctuations in time of the zonal mean (cell terms), the longitudinal fluctuations of the time average (standing eddies), and the zonal and time fluctuations (transient eddies). Each term and its contribution to the total variance with respect to longitude and time is computed and zonal Fourier and time spectral analysis is applied. For both seasons the total zonal-time variance remains at approximately the same magnitude from year to year as variability in standing eddy variance seems to be compensated by transient cell and eddy variance. Three significantly separated variance maxima in the wavenumber-frequency spectra are observed, which contribute to transient eddy variance. They occur in the ultra-long period and wavenumber range (k = 1 to 4, period $p \geqslant 12$ days), the long (k = 5–6, p = 5–12 days) and the short (k = 7 to 9, p = 4 to 5 days). In summer the peaks are shifted to higher wavenumbers. Zonally and time averaged transient eddy wave disturbances in the long and short wavenumber-period peaks show the typical vertical structure of east ward travelling baroclinic waves. Their phase speed can be approximated by Rossby wave dynamics. The ultra-long westward travelling waves (period $p \sim 20$ days) exhibit a quasi-barotropic vertical structure, thus giving no significant contribution to the meridional heat transport, while progressive waves of the same wavenumber and period resemble baroclinic waves and contribute to the meridional heat transport. These two wave modes seem to be adequate to explain the oscillations between high and low zonal index situations accompanied by blocking in the westwind zone.

Zusammenfassung: Kurze, lange und ultralange Störungen im Wellenzahl-Frequenzraum aus Beobachtungen auf dem Breitenkreis 50° N

Hemisphärische Geopotentialwerte entlang 50° N des Sommers 1969 und Winters 1969/70 sowie abgeleitete Schichtmitteltemperaturen und die Werte der meridionalen geostrophischen Windkomponente werden für troposphärische und zum Teil für stratosphärische Druckniveaus spektral analysiert, mit dem Ziel 1. eine Klimastatistik für Winter und Sommer zu erstellen, welche die bekannten makroturbulenten Prozesse der planetarischen Zirkulation in der Westwindzone beschreibt und 2. eine statistische Beschreibung der Raum-

1) on leave at: European Centre for Medium Range Weather Forecasts, Shinfield Park, Reading Berkshire RG2 9AX, United Kingdom

* Dedicated to Prof. Dr. H. Riehl on the occasion of his 65th birthday

0005-8173/80/01 0090-16 $ 02.00/0

und Zeitstruktur von zonal und zeitlich gemittelten Störungen in der nordhemisphärischen Westwindzone zu geben. Für das mittlere troposphärische Niveau 500 mb wird die Analyse auf 10 Winter (1969/70–1978/79) und 5 Sommer (1969, 1975–78) erweitert, um die Variabilität von Jahr zu Jahr zu ermitteln.

Nach zonaler und zeitlicher Mittelung läßt sich die Varaible q (λ, t) – z. B. geopotentielle Höhe, Temperatur oder meridionaler geostrophischer Wind – als Summe von vier Termen darstellen: durch das zeitliche und zonale Mittel und die zeitlichen Fluktuationen des zonalen Mittels (Zell-Terme), sowie die zonalen Fluktuationen des zeitlichen Mittels (ortsfeste Störungen) und die zonal-zeitlichen Fluktuationen (Wirbel-Terme). Alle Terme und ihre Beiträge zur totalen zonal-zeitlichen Varianz und zum gesamten meridionalen geostrophischen Temperaturtransport werden bestimmt und zonal Fourier und zeitlich spektral analysiert. In jedem Winter und Sommer gleichen sich die Abweichungen in den Varianzbeiträgen der ortsfesten und zeitlich fluktuierenden Störungen aus, so daß die totale zonal-zeitliche Varianz in jeder Saison von Jahr zu Jahr nahezu konstant bleibt. Zur Varianz der zonal-zeitlichen Fluktuationen werden aus drei signifikant getrennten Wellenzahl-Periodenbereichen maximale Beiträge geleistet: ultralang (Wellenzahl k = 1–4, Periode p ⩾ 12 Tage), lang (k = 5–6, p = 5–12 Tage) und kurz (k = 7–8, p = 4–5 Tage). Im Sommer werden Verschiebungen zu höheren Wellenzahlen beobachtet. Die zonal und zeitlich gemittelten transienten Wellenstörungen im lang- und kurzperiodischen Bereich haben die Struktur barokliner ostwärts wandernder Wellen, deren Phasengeschwindigkeit durch die Rossby-Wellendynamik gut beschrieben wird. Im ultralangperiodischen Bereich werden quasibarotrope westwärts wandernde Wellen (Periode ~20 Tage) beobachtet, die keinen signifikanten Beitrag zum meridionalen Transport fühlbarer Wärme leisten, und barokline nach Osten wandernde Wellen, durch die ein Wärmetransport nach Norden erfolgt. Diese Wellentypen sind geeignet, den Wechsel zwischen hohem und niedrigem Zonalindex und das Auftreten von Blockierungen in der Westwindzone zu erklären.

Résumé: Perturbations dans le domaine nombre d'ondes – fréquence d'après des observations à 50 °N de latitude.

Pour l'été de 1969 et l'hiver 1969–70, on a effectué une analyse spectrale du géopotentiel, de la température moyenne de certaines couches et du vent géostrophique méridien, le long du parallèle de 50 °N, à des niveaux de pression troposphériques et stratosphériques. Cette analyse visait à : 1:°) établir des statistiques climatiques pour l'hiver et l'été, qui décrivent les processus macroturbulents de la circulation planétaire dans la zone des vents d'ouest; 2:°) obtenir une description statistique, dans l'espace et le temps, de la structure des perturbations des latitudes moyennes de l'hémisphère nord, en moyenne zonale et temporelle. Au niveau de 500 mb, ces analyses sont étendues à 10 hivers (1969/70 à 1978/79) et 5 étés (1969, 1975–78) pour estimer la variabilité interannuelle.

En moyenne par rapport à la longitude et au temps, la variable q (λ, t) où q est le géopotentiel, la température ou le vent géostrophique méridien – est donnée par quatre termes: la moyenne temporelle et zonale, les fluctuations temporelles de la moyenne zonale (termes cellulaires), les fluctuations longitudinales de la moyenne temporelle (perturbations stationnaires), les fluctuations zonales et temporelles (pertubations transitoires). On calcule chaque terme et sa contribution à la variance totale par rapport à la longitude et au temps, et on applique l'analyse spectrale zonale et temporelle. Pour les deux saisons, la variance totale zonale – temporelle a le même ordre de grandeur d'année en année, la variabilité de la variance les perturbations stationnaires semble être compensée par la variance des cellules et perturbations transitoires. On observe trois maxima de variance, significativement séparés, dans les spectres en nombre d'ondes-fréquence, contribuant à la variance des tourbillons transitoires. Ces maxima apparaissent dans les gammes ultra-longue des périodes et nombres d'ondes (k = 1 à 4, période p ⩾ 12 jours), longue (k = 5 à 6, p = 5 à 12 jours) et courte (k = 7 à 8, p = 4 à 5 jours). En été, les pics sont décalés vers les plus grands nombres d'ondes. Les perturbations transitories, en moyenne zonale et temporelle, dans les pics de longue et courte période, révèlent la structure verticale typique des ondes baroclines se propageant vers l'est. Leur vitesse de phase est bien décrite par la dynamique des ondes de Rossby. Les ondes ultra-longues à déplacement vers l'ouest (période p ~20 jours) manifestent une structure verticale quasi barotrope, et ne contribuent donc pas significativement au transport méridien de chaleur, tandis que les ondes progressives des mêmes nombre d'ondes et période ressemblent à des ondes baroclines et contribuent au transport méridien de chaleur. Ces deux modes d'ondes semblent appropriés pour expliquer les oscillations entre les situations d'index élevé et bas accompagnées par un blocage dans la zone des vents d'ouest.

1 Introduction

Spectral analyses of local time series from rawinsonde data lead to statistical description of atmospheric phenomena and the dynamics of the synoptic scale. These observational statistics give additional aspects of the climatology of different climatic regions normally described by averages and variances. When spectral analysis in time and space is applied to hemispheric circulation data one has a powerful tool to compare the dynamics of model atmospheres with the observed circulation in an objective way. Additionally, quantitative measures are obtained to characterize the synoptic situation of a season. In a recent paper (FRAEDRICH and BÖTTGER, 1978) it was found by spectral decomposition of observed geopotential zonal-time fluctuations along a mid-latitude circle in winter that three defined ranges in the wavenumber-frequency domain contribute to the total transient eddy variance: ultra-long waves (wavenumber k = 1 to 4) are quasi-standing oscillations with periods $p > 12$ days, long waves (k = 5 to 6) and short waves (k = 7 to 8) propagate eastward with periods p = 5 to 12 and $p < 5$ days, respectively. Similar peaks were found by HAYASHI and GOLDER (1977) for model output data of the GFDL circulation model.

But, transient eddy variance is only one part of the total zonal-time variance. When averaged with respect to longitude and time any variable $q(\lambda, t)$ is given by four terms

$$q(\lambda, t) = [q]_{\lambda,t} + ([q]_\lambda)_t + ([q]_t)_\lambda + (q)_{\lambda,t} \tag{1.1}$$

with the time and zonal averages $[\ ]_t$, $[\ ]_\lambda$ and the related departures $(\ )_t$, $(\ )_\lambda$ (adopted from REITER, 1969). The first term on the right hand side is the zonal-time average attributed to the mean meridional circulation (standing cell), the second term represents the fluctuations in time of the zonal mean (transient cell), the third the longitudinal fluctuations of the time averages (standing eddies) and finally the fourth term represents the zonal and time fluctuations (transient eddies). Only the last three terms contribute to the total zonal-time variance.

$$\text{Var } q(\lambda, t) = [([q]_\lambda)_t^2]_{\lambda,t} + [([q]_t)_\lambda^2]_{\lambda,t} + [(q)_{\lambda,t}^2]_{\lambda,t} \tag{1.2}$$

because $[q^2]_{\lambda,t} = [q]_{\lambda,t}^2 + \text{Var } q(\lambda, t)$. In the same way the zonal and time averaged meridional transport of the variable q across a latitude circle is obtained.

$$[vq]_{\lambda,t} = [v]_{\lambda,t}[q]_{\lambda,t} + [([v]_\lambda)_t ([q]_\lambda)_t]_{\lambda,t} + [([v]_t)_\lambda ([q]_t)_\lambda]_{\lambda,t} + [(v)_{\lambda,t} (q)_{\lambda,t}]_{\lambda,t} \tag{1.3}$$

where the meaning of the transport terms is analogous to Equation (1.1).

The aim of this paper is a) to establish climatic circulation statistics for winter and summer which describe the known macro-turbulent processes of the planetary circulation in the westwind zones and b) to obtain a statistical description in the space-time domain of zonally and time averaged mid-latitude disturbances of the Northern Hemisphere. First, the method of analysis will be presented in Section 2. Section 3 deals with each contributing term of (1.1) to the total zonal-time variance and the year-to-year variability. Then in section 4 transient eddy variance is decomposited in the wavenumber-frequency domain to determine the dominating scales of time fluctuating atmospheric processes causing weather and seasonal climatic variability. Finally, the vertical structure of disturbances in the three dominant scales is discussed to achieve further insight in the behaviour of the zonal waves and their motion, and the related transport processes, which make up the mid-latitude general circulation.

2 Data and method of analysis

To determine the macro-turbulent processes of the Northern Hemisphere westwind zones the analyses are carried out along 50° N. At this latitude circle the zonally and time averaged transient eddy

variance of the meridional wind and the related energy transports achieve their maximum (OORT and RASMUSSON, 1971). For summer 1969 and winter 1969/70 daily geopotential height values Z are taken from standard level hemispheric charts on a 10 degree longitude grid around 50° N (36 points). Thus, the scale of the smallest eddy resolved will be about 1500 km. The pressure levels chosen are 1000 mb (surface), 850, 500, 300, 200 and 100 mb. Data sets for both seasons have an equal length of 120 days beginning on 1 May and 1 November. This is in agreement with time series analyses of the Berlin rawinsonde (FRAEDRICH, BÖTTGER and DÜMMEL, 1979); though station soundings allow a much better resolution with height. For all pressure levels the meridional geostrophic wind component V_g and for all relative topographies the mean temperature distribution can be derived by using the hydrostatic relation. At the 500 mb level the analyses are extended to ten winters (1969/70–78/79) and five summers (1969, 1975–78) to qualitatively judge the confidence of conclusions drawn from finite sample statistics and to have an estimate of the year-to-year variability. The data analysed are digitized from daily hemispheric charts at the Meteorologisches Institut, Freie Universität Berlin, of the Deutscher Wetterdienst and the weather service of the USSR.

For each data set (36 grid points x 120 days) all the terms contributing to the total variance (1.2) are determined. Then by applying zonal Fourier and time spectral analyses the transient eddy variance is decomposited in the wavenumber-frequency domain following the procedure described by HAYASHI (1971, 1973). Transient eddy variance is due to fluctuations with respect to time and longitude and can be interpreted by a composition of progressive (−f) and retrogressive (+f) waves of discrete wavenumber k and frequency bands Δf centered at f:

$$[(Z)^2_{\lambda,t}]_{\lambda,t} = \sum_{k=0}^{\infty} \sum_{f=0}^{\infty} \{E_z(k,+f) + E_z(k,-f)\} \tag{2.1}$$

$E_z(k, \pm f)$ is the two-sided variance density spectrum of geopotential Z in the wavenumber-frequency domain and can be obtained by first expanding $(Z)_{\lambda,t}$ to zonal Fourier harmonics and then computing the power-, co- and quadrature spectra of the cosine and sine components. The propagating variance density spectrum PR (k, f) ist defined by the difference of the eastward and westward contribution of (2.1) and equals the quadrature spectrum Q_f:

$$PR(k,f) = |Q_f(C_k, S_k)| \tag{2.2}$$

The propagation direction can be inferred from the algebraic sign of Q_f. True time fluctuations at a fixed longitude (stationary fluctuations), resulting from waves of the same wavenumber- and frequency band travelling in opposite directions, can only be determined, if the coherence between these waves is close to 1.0 (PRATT, 1976).

Stationary variance can be given by the difference between the total and propagating part of transient eddy variance, even if the coherence is not close to 1.0, when, for example, practically no westward travelling waves exist in a frequency band (HAYASHI, 1977). No further effort was made to separate true wave motions from the total variance (for further discussion of this method see SCHÄFER, 1979). The Fourier harmonics are cut off at wavenumber k = 12, beyond which the remaining zonal variance appeared to be negligibly small (<5 %). The residual variance can be regarded as noise considering the time steps and the zonal grid spacing. The spectra are computed by using a lag-correlation method with a 20-day lag. Smoothing is accomplished by applying the Tukey lag window with an equivalent band width of b = .665 cpd and approximately 15 degrees of freedom for each of the 41 spectral estimates. Both in summer and winter the zonal and time fluctuations showed almost no trend; therefore, it was not removed.

3 Total zonal-time variance of geopotential

Throughout the troposphere the total zonal-time variance of geopotential height increases, reaching its maximum just below the tropopause. At all levels the three variance terms in Equations (1.2) contribute to the total variance at the same rate (BÖTTGER, 1979). Thus, the main features can be shown by concentrating on the computed variance terms at the 500 mb level for the five summer and seven winter seasons (Table 1 and 2).

■ **Table 1** Zonal-time variance of geopotential at 500 mb and 50 °N for five summer seasons and their average. Propagating variance is part of the transient eddy variance, percentage given in brackets; units of geopotential: gpdam, units of variance terms: gpdam^2.

■ **Tabelle 1** Zonal-zeitliche Varianz des Geopotentials in 500 mb und auf 50 °N für fünf Sommer und das Mittel. Die Varianz der wandernden Störungen ist Teil der Varianz der transienten Störungen, prozentualer Anteil in Klammern. Einheiten des Geopotentials: gpdam; Einheiten der Varianzterme: gpdam^2.

Year	Zonal-time mean of geopotential	Variance of transient cell	Variance of standing eddies	Variance of transient eddies	Propagating variance	Total variance of zonal-time fluctuations
1969	563.4	62.9	16.7	80.6	29.6 (37%)	160.2
1975	565.7	43.8	17.0	63.0	20.2 (32%)	123.8
1976	563.8	41.5	24.2	69.5	27.8 (40%)	135.2
1977	564.6	35.8	14.4	76.8	26.7 (35%)	127.0
1978	565.2	39.5	9.4	76.5	30.2 (39%)	125.4
average	564.5	44.7	16.3	73.3	26.9 (37%)	134.3

■ **Table 2** Zonal-time variance of geopotential at 500 mb and 50 ° N for ten winter seasons and their average. Propagating variance is part of the transient eddy variance, percentage given in brackets; units of geopotential: gpdam, units of variance terms: gpdam^2.

■ **Tabelle 2** Zonal-zeitliche Varianz des Geopotentials in 500 mb und auf 50 ° N für zehn Winter und das Mittel. Die Varianz der wandernden Störungen ist Teil der Varianz der transienten Störungen, prozentualer Anteil in Klammern. Einheiten des Geopotentials: gpdam; Einheiten der Varianzterme: gpdam^2.

Year	Zonal-time mean of geopotential	Variance of transient cell	Variance of standing eddies	Variance of transient eddies	Propagating variance	Total-variance of zonal-time fluctuations
1969/70	536.6	40.5	143.1	148.3	56.8 (38%)	331.9
1970/71	537.9	30.7	85.2	181.7	67.2 (37%)	297.6
1971/72	537.5	43.5	106.7	156.4	59.6 (38%)	306.6
1972/73	537.7	22.3	116.5	162.5	54.5 (34%)	301.3
1973/74	537.2	31.3	94.4	177.3	66.5 (38%)	303.3
1974/75	537.4	20.6	130.0	128.6	42.8 (33%)	279.2
1975/76	539.2	33.6	113.2	176.9	73.6 (42%)	323.7
1976/77	534.4	28.7	187.6	127.4	47.0 (37%)	343.7
1977/78	536.4	35.1	107.8	161.4	54.4 (34%)	304.3
1978/79	537.0	47.5	94.3	151.4	65.7 (43%)	293.2
average	537.1	33.4	117.9	157.2	58.8 (37%)	308.5

Total variance in summer is at a much lower level than during winter, though both seasons exhibit the same characteristics. Only small deviations from its average value can be observed for the total zonal-time variance, while the individual terms exhibit a much larger variability. Variance due to time fluctuations of the zonal average (transient cell $[([Z]_\lambda)^2_t]_{\lambda,t}$) is largely caused by the seasonal warming and cooling, it is larger in summer than in the winter period, but does not change much from year to year. Time averaged disturbances (standing eddies $[([Z]_t)^2_\lambda]_{\lambda,t}$ and fluctuations in time (transient cell $[([Z]_\lambda)^2_t]_{\lambda,t}$ plus transient eddies $[(Z)^2_{\lambda,t}]_{\lambda,t}$) seem to compensate each other for each season. When standing eddy variance is high (time averaged climatological trough and ridges along 50 °N are well pronounced) the transient cell plus transient eddy variance tends to be reduced. On the other hand time dependent fluctuations contribute at a higher rate in seasons with relatively low standing eddy variance. The propagating variance PR (k, f) as a part of the transient eddies can be attributed to travelling waves and is in summer and winter given by a nearly constant fraction of 37 % of the total transient eddy variance. Thus, mainly disturbances which are quasi-standing oscillations will amplify. They cause atmospheric pulsations at fixed longitudinal locations on the latitude circle, observed by the index or vacillation cycle. Numerical experiments with a general circulation model confirm this atmospheric behaviour: Mountains tend to produce downwind standing eddies while, when the orographic barriers are left out, transient eddy activity is enhanced. But, for both cases the total zonal-time variance is hardly effected (MANABE and TERPSTRA, 1974).

Especially in the winter, variance terms of standing eddies and transient cell plus transient eddies indicate a quasi-biennual cycle: however, with only a small sample of ten winters no statistical significance can be given. In years with enhanced standing eddy variance the meridional type of circulation will prevail in the westwind zones, otherwise zonality will be more frequent. This is confirmed by BÖHME (1967) who found a 26-month cycle in the frequency of days with prevailing meridional circulation patterns over Europe. His analysis is based on the classification of Großwetterlagen (HESS and BREZOWSKY, 1977).

4 Variance of zonal-time fluctuations (transient eddies)

In this section a spectral decomposition of transient eddy variance of the geostrophic meridional wind $[(V_g)^2_{\lambda,t}]_{\lambda,t}$ is presented to determine the dominant scales in time and space of the atmospheric motions in the mid-latitudes. The variance of the geostrophic wind component is proportional to the macro-turbulent kinetic energy of the meridional component of the transient eddies. The spectra are shown in linear wavenumber-frequency diagrams: The frequency axis is labelled in periods p of days, while the upper abscissa gives the related phase velocity $C = Lp^{-1}$ in ms^{-1}; L is the wavelength of the hemispheric wave at 50 °N. The isolines of the phase velocity C converge at wavenumber $k = 0$ and $p = \infty$. The spectral estimates computed for discrete wavenumbers k and frequencies f are then interpolated linearily, and in addition smoothed out manually, leaving the main features of the spectra unchanged. No filter technique has been applied to isolate or stress atmospheric processes in a certain wavenumber or frequency range; thus, the spectra represent the variance caused by all atmospheric motions resolved by the data.

Two wavenumber-frequency diagrams show the average conditions for the five summer – 1969 and 1975 to 1978 – and ten winter seasons – 1969/70 to 1978/79 – (Figures 1 and 2). The maxima contributing to the total transient eddy variance of the meridional geostropic wind V_g at 500 mb along 50 °N are arranged in a band orientated from small wavenumbers and ultra-long periods to large wavenumbers and short periods. A line connecting these spectral peaks results in a "dispersion line", which describes the change in phase velocity as a function of wavelength or wavenumber. Along this dispersion line three separated peaks in the spectra can be seen. They suggest the following division of the atmo-

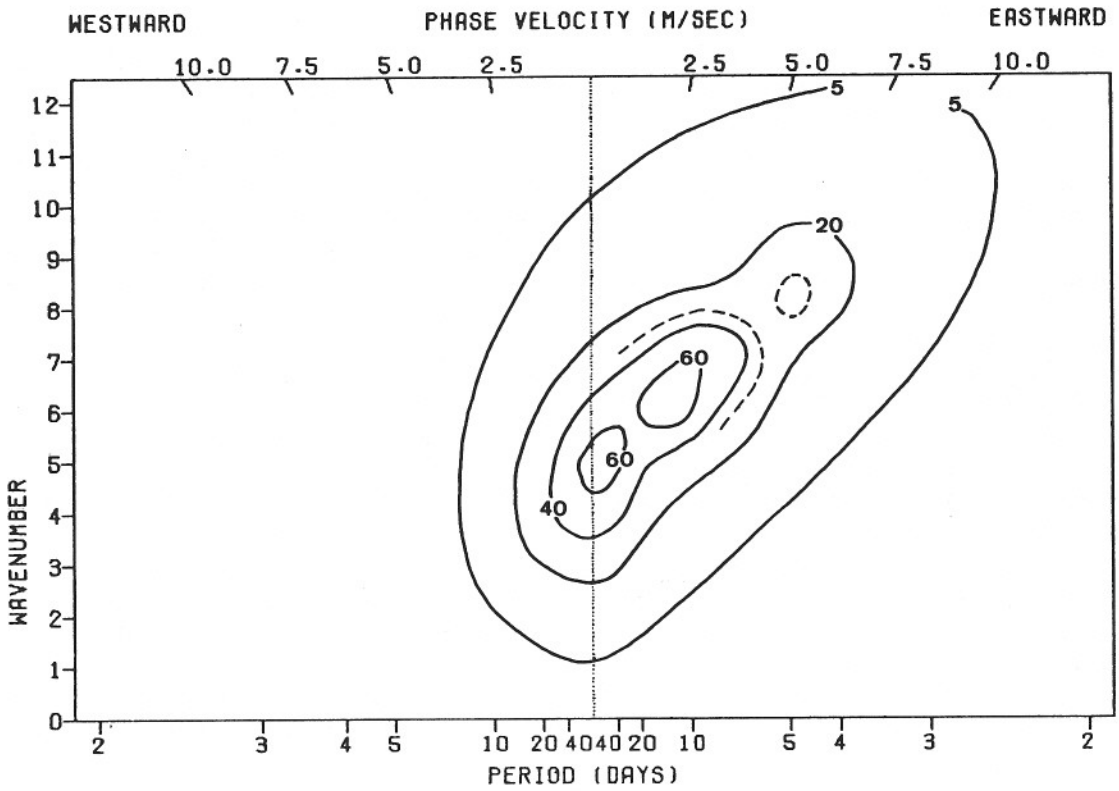

- **Figure 1** Wavenumber-frequency contours of power spectrum density ($m^2 s^{-2}/\Delta f$) of the meridional geostrophic wind at 500 mb along 50 °N for the summer average (Δf = .025 cpd, but Δf = .0125 cpd for f = 0 and f = .5 cpd).

- **Bild 1** Wellenzahl-Frequenz-Spektrum der Varianzdichte-Verteilung ($m^2 s^{-2}/\Delta f$) der Meridionalkomponente des geostrophischen Windes in 500 mb auf 50° N für das Sommermittel (Δf = .025 cpd, aber Δf = .0125 cpd für f = 0 und f = .5 cpd).

spheric motion processes into three main ranges of macro-turbulent activity in the wavenumber-frequency domain for the winter season with the variance minima defining the scale-related wavenumber and period intervals.

(i) "Short period" fluctuations are associated with short (minor) waves (period $p < 5$ days, wavenumber k = 7 to 8), fast travelling eastward with a phase velocity $c \geqslant 8\ ms^{-1}$.

(ii) "Long period" variability is caused by long (major) waves (p = 5 to 12 days, k = 5 to 6) slowly propagating eastward with a phase velocity c = 4 to 7 ms^{-1}.

(iii) "Ultra-long period" processes are related to the ultra-long waves ($p > 12$ days, k = 1 to 4), which are quasi-stationary but fluctuating in time.

In summer a shift to somewhat higher wavenumbers is observed, leaving the three period ranges unchanged. The scale in space of the macro-turbulent eddies is smaller, due to the reduced zonal mean flow. This classification of disturbances along 50 °N is in good agreement with a single-station climatology for Berlin (52 °N, 13 °E) based on 12 years aerological soundings (FRAEDRICH et. al., 1979). Thus, locally observed time spectra and their dominant time scales can be related to hemispheric waves in the westerlies

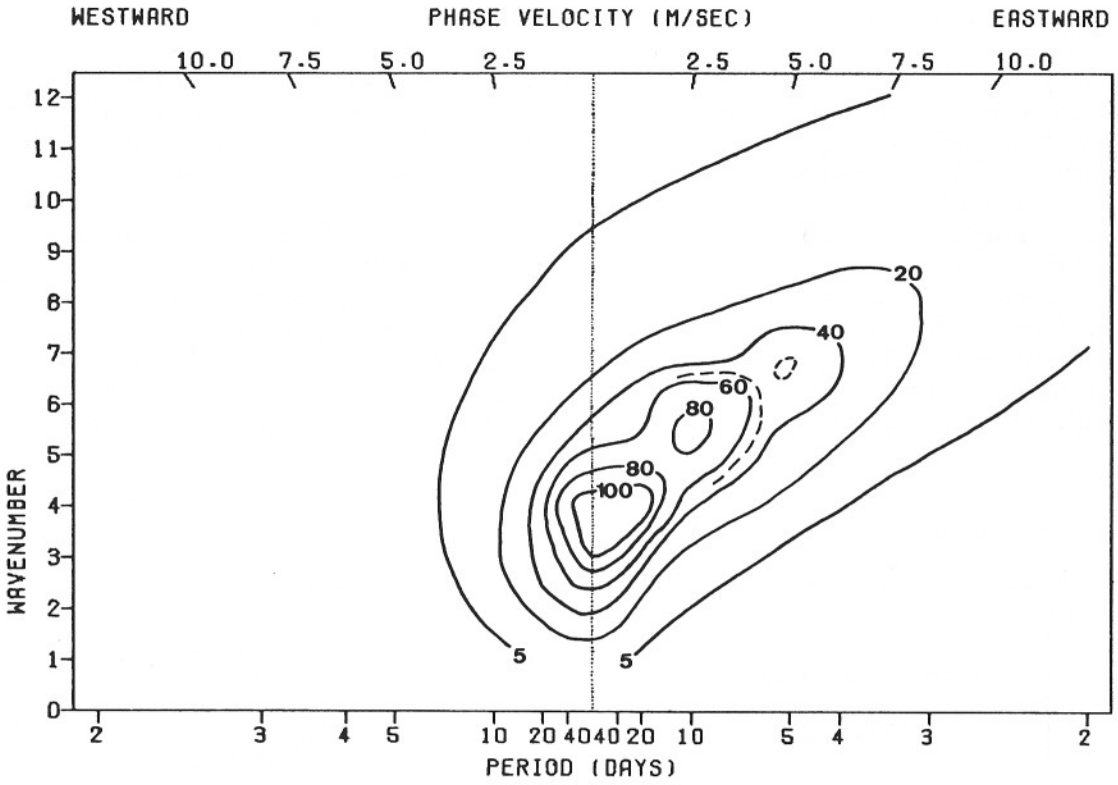

- **Figure 2** Wavenumber-frequency contours of power spectrum density ($m^2 s^{-2}/\Delta f$) of the meridional geostrophic wind at 500 mb along 50° N for the winter average. (Δf = .025 cpd, but Δf = .0125 cpd for f = 0 and f = .5 cpd.).

- **Bild 2** Wellenzahl-Frequenz-Spektrum der Varianzdichte-Verteilung ($m^2 s^{-2}/\Delta f$) der Meridionalkomponente des geostrophischen Windes in 500 mb auf 50° N für das Wintermittel (Δf = .025 cpd, aber Δf = .0125 cpd für f = 0 und f = .5 cpd.).

(see also FIEDLER, 1971). For each individual season the spectra have been tested against a first order Markov process as "Null"hypothesis having the same total variance. The spectral peaks exceed the red-noise spectra by a factor of 2 to 2.5. Significance seems to be well established with 15 degrees of freedom and a priori significance level of 95 % based on prior knowledge of related observations and similar model output interpretation (see e. g. HAYASHI and GOLDER, 1977).

The largest contributions to the total transient eddy variance come from the ultra-long period and wave-number fluctuations observed at the low frequency end of the spectra where averaging over a wide period range occurs. As the waves in the same frequency band travelling to the east and to the west are hardly coherent with each other (PRATT, 1976), no true standing wave motion, i. e. fluctuations in time at fixed locations along 50 °N can be expected. The westward travelling (retrogressive) geopotential waves exhibit a slightly larger amplitude than the progressive waves in the ultra-long period range, while quadrature spectrum analyses of hemispheric temperature fields reveal that the opposite holds for the temperature waves (KAO, 1970; WILLSON, 1975, PRATT and WALLACE, 1976). It can therefore be expected that the zonal-time fluctuations in the ultra-long period range are caused by ultra-long progessive and retrogressive waves of different vertical structure (Section 5).

The variance contributions in the long and short-period range are limited to the eastward travelling progressive long and short waves. Their phase speed can approximately be determined from the Rossby formula $C_R = \overline{U} - \beta L^2/4\pi^2$ for travelling waves in a barotropic non-divergent atmosphere with infinite lateral boundaries. The average zonal wind $\overline{U}$ has to be taken in the level of non-divergence not far from the 500 mb level. From the surface up to the tropopause $\overline{U}$ increases with height, but the spectral peaks computed at all available pressure levels for winter 1969/70 and summer 1969 remain at the same position in the wavenumber-frequency domain throughout the troposphere (BÖTTGER, 1979). Thus, the travelling waves are highly coherent with each other at all levels (DELAND, 1973). The dispersion lines of the winter and summer spectra at 500 mb, which is the steering level for the wave propagations, are shown in Figure 3. They nearly coincide with the phase speed lines derived from the Rossby formula, where $\overline{U}$ = 15 m sec^{-1} and $\overline{U}$ = 10 m sec^{-1} are the longitudinally averaged zonal wind components for winter and summer at 500 mb in 50 °N. Though the Rossby phase velocity can only be the lower limit as divergence effects and lateral boundaries tend to increase the speed of propagation, the propagation of the zonally averaged synoptic scale long and short wave disturbances can approximately be described by the Rossby wave

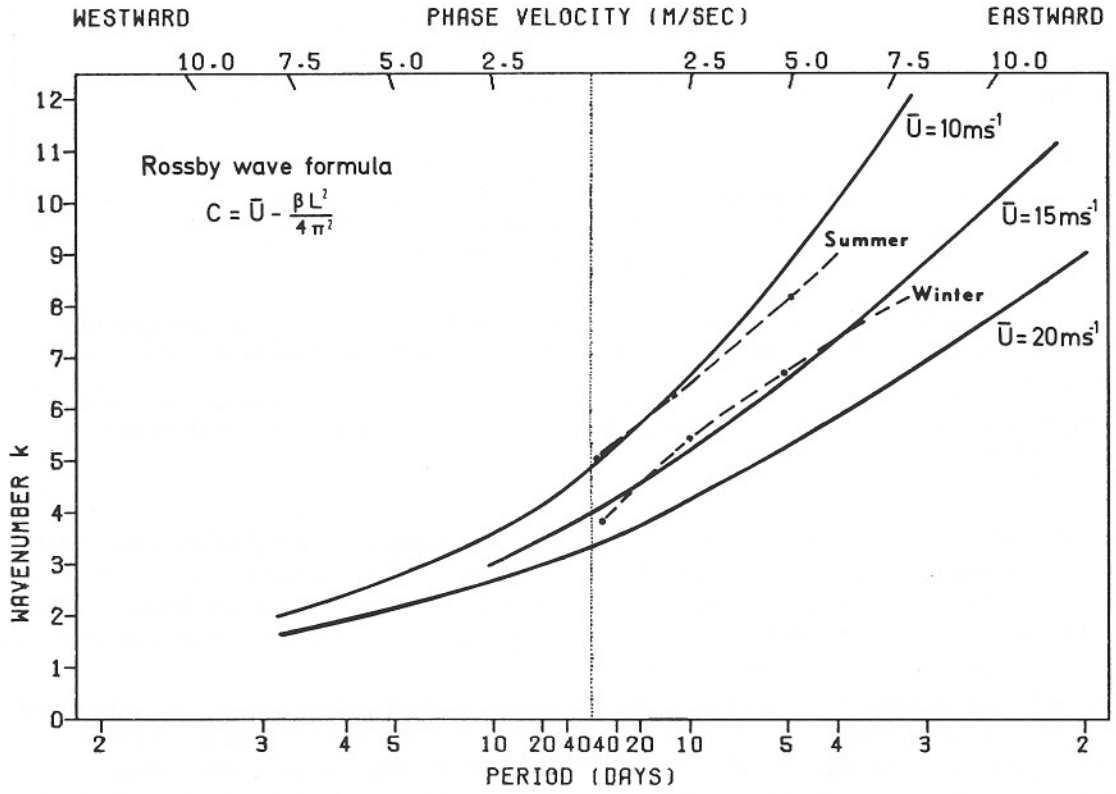

- **Figure 3** Phase velocity C_R (full lines) of Rossby waves at 50 °N for different values of the zonal flow $\overline{U}$. Wavelength L depending on wavenumber k, "dispersion lines" from summer and winter spectra (dotted lines).

- **Bild 3** Phasengeschwindigkeit C_R (durchgezogen) von Rossby-Wellen auf 50 °N für verschiedene Werte des zonalen Grundstroms $\overline{U}$. Die Wellenlänge L hängt ab von der Wellenzahl k, „Dispersionslinien" der Sommer- und Winterspektren (gestrichelt).

■ **Table 3** Variance (gpdam²) of geopotential for transient eddies at 50 °N and 500 mb, integrated over the short, long and ultra-long period range for ten winter seasons and the average.

■ **Tabelle 3** Varianz (gpdam²) des Geopotentials für transiente Störungen in 500 mb auf 50 °N integriert über den kurz-, lang- und ultralangperiodischen Bereich für zehn Winter und das Mittel.

Year/Period	ultra-long $p > 12$ days	long $p = 12$ to 6 days	short $p < 6$ days
1969/70	101	30	18
1970/71	131	29	21
1971/72	100	31	25
1972/73	109	28	25
1973/74	123	30	24
1974/75	87	24	18
1975/76	114	35	28
1976/77	79	27	22
1977/78	111	29	21
1978/79	102	29	20
average	106	29	22

dynamics. These processes, however, contribute only a small amount to the transient eddy variance, most of which is due to ultra-long period fluctuations superimposed on the standing eddies with k = 1 to 4 in winter and k = 1 to 5 in summer.

When averaged over ten winter or five summer seasons the three spectral peaks remain separated, although there is a large year-to-year variability in each of the period ranges (Table 3). Its magnitude remains largest for the ultra-long periods and waves. In single-station rawinsonde spectra the ultra-long and long-period ranges can sometimes hardly be separated, especially when they are averaged over many years (FRAEDRICH et. al., 1979). Obviously, a reduction in standing eddy variance is mainly compensated by transient eddy variance of the ultra-long waves which then is accompanied by enhanced activity of the long and short wavenumber and period disturbances. However, such a relation between standing and transient eddy variance may be partly due to the chosen length and period of the time series, though tests with shifted and shortened time series (up to one month) gave evidence of minor effects on the spectra.

5 Vertical structure of transient wave disturbances

The vertical and horizontal phase relationships of these waves will be presented and some aspects of the interactions between the wave disturbances in the three wavenumber-period ranges will be outlined. The procedure to calculate the wavenumber and frequency dependent phase relationship $\phi'_{k,\pm f}$ between travelling waves $W_k(\lambda, t)$ and $W'_k(\lambda, t)$ at two different pressure levels p and p′ is described by HAYASHI (1971). It is basicly a multiple cross-spectrum analysis applied to the time series of the sine and cosine coefficients $S_k(t)$ and $C_k(t)$, $S'_k(t)$ and $C'_k(t)$ belonging to these waves.

$$\phi'_{k,\pm f} - \phi_{k,\pm f} = \arctan \{Q_{\pm f}(W_k, W'_k)/K_{\pm f}(W_k, W'_k)\}$$

where

$$4\,K_{\pm f}(W_k, W'_k) = K_f(C_k, C'_k) + K_f(S_k, S'_k) \pm Q_f(C_k, S'_k) \mp Q_f(S_k, C'_k)$$

$$4\,Q_{\pm f}(W_k, W'_k) = \pm Q_f(C_k, C'_k) \pm Q_f(S_k, S'_k) - K_f(C_k, S'_k) + K_f(S_k, C'_k)$$

The reliability of the results can be judged in a similar way as pointed out by FRAEDRICH et al. (1979) for the locally observed short period disturbances at Berlin. The squared coherence

$$\mathrm{Coh}^2_{\pm f}(W_k, W'_k) = \frac{K^2_{\pm f}(W_k, W'_k) + Q^2_{\pm f}(W_k, W'_k)}{P_{\pm f}(W_k)\,P_{\pm f}(W'_k)}$$

can be computed as a measure of the similarity between the waves at two pressure levels p and p′. This is important as frequency band averaging is applied, and if the coherence drops under a lower confidence limit the phase relationship might not be too meaningful. This limit depends on the chosen a priori probalility level α and the degrees of freedom v (d.o.f.) (MWO, 1966):

$$(\mathrm{Coh}^2)_{\mathrm{sign}} \sim \{1 - (1-\alpha)^{1/(v-1)}\}^{1/2}$$

Then a phase error can be placed on the estimated phase $\phi'_{k,\pm f} - \phi_{k,\pm f}$ depending on the same variables

$$\sin^2 \Delta\phi = \frac{1 - \mathrm{Coh}^2}{\mathrm{Coh}^2}\left[(1-\alpha)^{-2/v} - 1\right]$$

Computing the phase lines and the amplitudes for the short wave disturbances a band averaging over four adjacent frequency points has been applied covering the period from 4 to 6 days. This gives v = 61 d.o.f. and at a given 95 % significance level a $(\mathrm{Coh}^2)_{\mathrm{sign}} = .22$, indicated by arrows in Figures 4 and 5. With a computed coherence well above this lower limit the statistical results appear to be significant. An observed squared coherence of $\mathrm{Coh}^2 = .8$ would mean a phase error of less than 10°.

In the ultra-long period range only one frequency point was used covering the period 16 to 27 days. With v = 15 d.o.f. and $(\mathrm{Coh}^2)_{\mathrm{sign}} = .43$ at the 95 % level this means a phase error of more than 50°. Especially the temperature phase lines prove to be hardly significant. Still, the vertical structures of the eastward and westward travelling ultralong waves will be presented, as they seem to be physically meaningful. But there is a need to further check the results by extending the statistics. The following figures are only presentations of single season realizations for winter (1969/70) and summer (1969).

Figure 4 shows the internal structure of the synoptic scale disturbances producing the zonal-time fluctuations along the 50 °N latitude circle in the short wavenumber-period range, period p = 5 days and wavenumber k = 7 in winter and k = 9 in summer: The vertical tilt of the axes of geopotential height (Z_{max}, Z_{min}), geostrophic meridional wind (V_{max}, V_{min}), and temperature (T_{max}, T_{min}), their phase differences, their amplitudes, and the squared coherences. All phases and the coherences are computed with respect to the geopotential waves at 850 mb. Both the winter and summer disturbances exhibit the same features. The vertical axes of the troughs and ridges show a remarkable westward tilt with height in the lower troposphere. The slope gradually decreases around 500 mb. Above this level the geopotential waves are almost in phase. Only a slight forward tilt of the temperature axes is observed throughout the troposphere. Thus, they approach the trough and ridge lines without crossing them before a phase jump occurs at the mean height of the tropopause, where the amplitudes of the geopotential waves and the related wind achieve their maximum. At the same level the temperature wave has its smallest amplitude and is poorly correlated with the geopotential wave near the surface (at 850 mb) according to the low coherence value. As the phase lag between the temperature and wind waves never exceeds 90° in the troposphere, the geostrophic meridional transport of sensible heat performed by short wave disturbances is always positive. This holds for the zonally averaged disturbances, where all stages of development are taken into consideration. Speth's (1974) computations of the vertically averaged meridional sensible

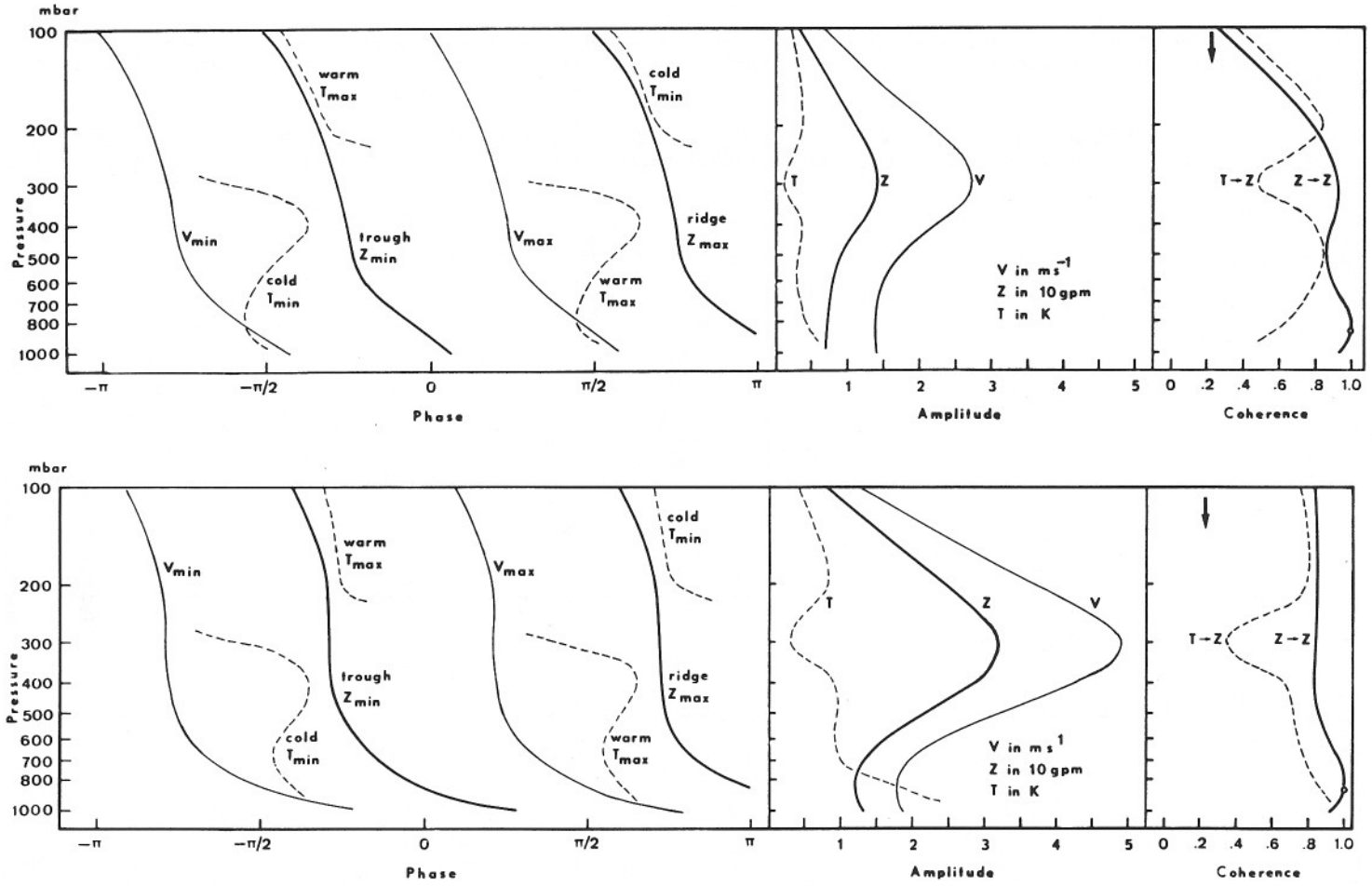

● **Figure 4** Diagramm of phase relationships, amplitudes and coherences of meridional geostrophic wind V, geopotential height Z and temperature T for short period progressive wave disturbances, period p = 5 days, along 50 °N, top: summer 1969, wavenumber k = 9; bottom: winter 1969/70, k = 7.

● **Bild 4** Phasenbeziehungen, Amplituden und Kohärenzen zwischen geostrophischem meridionalen Wind V, geopotentieller Höhe Z und Temperatur T für kurzperiodische progressive Wellenstörungen, Periode p = 5 Tage, entlang 50 °N, oben: Sommer 1969, Wellenzahl k = 9; unten: Winter 1969/70, k = 7.

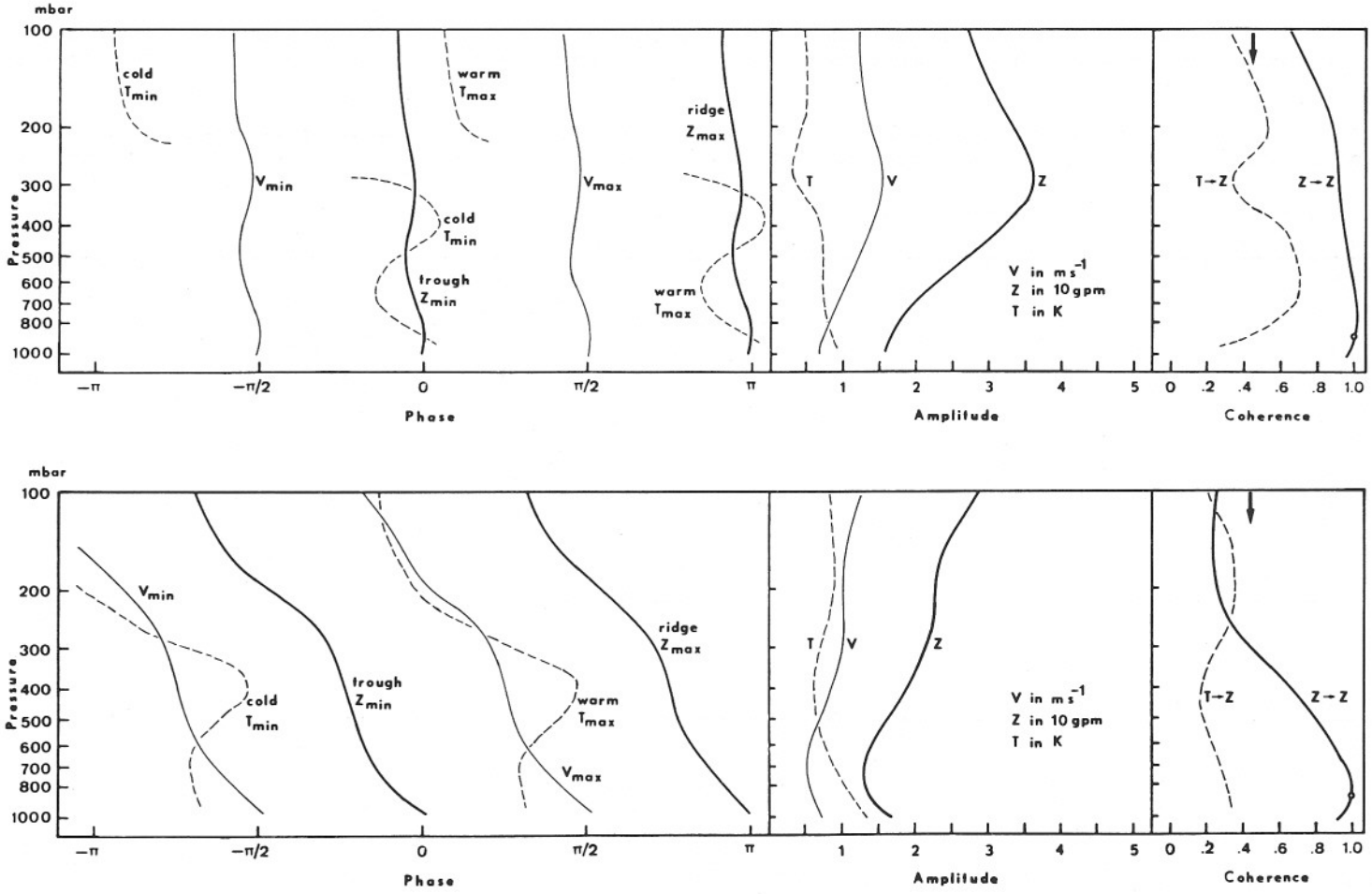

- **Figure 5** Diagram of phase relationships, amplitudes and coherences of meridional geostrophic wind V, geopotential height Z and temperature T for ultra-long period wave disturbances, period p = 20 days, wavenumber k = 2, along 50 °N in winter 1969/70; top: westward, bottom: eastward travelling wave.

- **Bild 5** Phasenbeziehungen, Amplituden und Kohärenzen zwischen geostrophischem meridionalen Wind V, geopotentieller Höhe Z und Temperatur T für ultra-langperiodische Wellenstörungen, Periode p = 20 Tage, Wellenzahl k = 2, entlang 50 °N im Winter 1969/70; oben: westwärts, unten: ostwärts wandernde Wellen.

heat transport by transient eddies over the northern hemisphere gave large flux values over areas with enhanced baroclinic activity, while smaller values or even a southward transport of heat occurs over areas such as the eastern Pacific and western coast of North America or Europe where disturbances in a mature, occluded stage are observed frequently. They cause a negative heat transport in the upper tropospheric levels in the short period range, though the vertically averaged flux is still positive as it has been documented by mid-latitude single station climatology statistics (MÜLLER, BUCHWALD and FRAEDRICH, 1979).

As the ultra-long period eastward and westward travelling waves k = 2 for summer and winter exhibit similar features only the internal structure of the waves for the winter season 1969/70 will be presented. The retrogresssive wave, k = 2, p = 20 days (Figure 5, top), shows hardly any vertical tilt of the troughs and ridges, and their phase lines coincide with the axes of the warm and cold air taking the phase error into consideration. Thus, the phase lag between the temperature and the wind wave is nearly 90° throughout the troposphere and no contribution to the total transport of sensible heat by transient eddies can be expected. The eastward travelling wave (k = 2, p = 20 days), at the bottom of Figure 5, exhibits some features of a baroclinic wave. Troughs and ridges tilt westward with height and the eastward tilting axes of the temperature waves lag the geopotential phase lines, so that a positive sensible heat transport is performed by this wave mode. At the tropopause level no phase jump in temperature is observed but only a steep slope in the westward tilting phase line. Thus, these waves can support the increase of turbulent kinetic energy in the stratosphere, as westward tilting axes of geopotential waves lead to an upward transport of wave energy (geopotential flux) (ELIASSEN and PALM, 1961). The retrogressive ultra-long wave k = 2 with its steep vertical structure does not transport any energy from the troposphere into the stratosphere. SATO (1977) found that this wave even tilts forward in the stratosphere giving a downward transport of wave energy.

In summary, there exist two distinct wave modes in the ultra-long wavenumber- and period range: The progressive wave k = 2, p = 20 days, resembles a baroclinic wave pattern. It makes positive contributions to the meridional sensible heat transport and to the vertical wave energy transport. Thus, it helps to decrease the mid-latitude meridional temperature gradient and to increase the turbulent kinetic energy at higher levels. The retrogressive wave k = 2, p = 20 days, looks more like a barotropic wave. It neither contributes to the meridional temperature transport nor to the geopotential flux. HUNT (1978) has traced these two wave modes in vacillation cycles of a model atmosphere. Baroclinic activity in the ultra-long period range is accompanied by enhanced baroclinic activity in the long and short period range as follows. The pronounced meridional flow will produce warm blocking anticyclones in higher latitudes and cut-off lows in the south, which automatically reduce the latitudinal temperature gradient. This episode is then followed by a period of "quiet" baroclinic activity during which the atmosphere prefers the observed retrogressive ultra-long wave mode, thus allowing the latitudinal temperature gradient to be established again by radiation processes, while the poleward flux of heat is small. Then the index or vacillation cycle repeats itself. It is possible to compute the phase difference in time for the two ultra-long waves at a fixed location on the latitude circle. It shows consistency with height, but without much statistical reliability. Generally speaking, when the locally observed phase difference is found to be small, the progressive ultra-long wave ridge will at the same position soon be followed by the retrogressive wave maximum. Thus, a blocking situation will be more pronounced over this area, while upstream and downstream, where the phase difference between the two ultra-long waves is increasing, a more flattish circulation pattern can be expected.

6 Final remarks

Single-station climatology of different climatological areas has been complimented by this study giving climatological statistics of the macro-turbulent midlatitude disturbances. Additional insight has been gained into inherent features of the general circulation such as the vacillation cycle or the scale related hierarchy of macro-turbulent processes, thereby corroborate the interpretations from single-station observations. These dominating wavenumber and frequency scales are related to circulation stages in the mid-latitudes of the northern hemisphere, extensively described by RIEHL et. al. (1952). Furthermore, these statistical methods are a powerful tool to test and verify the dynamical processes produced by numerical models. By establishing ensemble statistics for all forecast days produced daily, it can be possible to detect deficiencies in the model dynamics and to trace these to the wavenumber-frequency range which is most affected.

Acknowledgement

Thanks are due to JOHN E. KUTZBACH, University of Wisconsin, Madison, for stimulating discussion, to MARTINA SCHOLZ, HOLGER HAUG and ULLA ECKERTZ-POPP for typing, drawing, and photographing. Computations and plotting were carried out at the Zentraleinrichtung für Datenverarbeitung (Zedat), F.U. Berlin.

Dieser Beitrag zum 65sten Geburtstag von HERBERT RIEHL vermag nur in geringem Maß das auszudrücken, was während unserer Begegnungen in Anaco, Fort Collins und Berlin entstehen konnte.

References

BÖHME, W., 1967: Eine 26-monatige Schwankung der Häufigkeit meridionaler Zirkulationsformen über Europa. Z. Meteor., **19**, 113–115.

BÖTTGER, H., 1979: Spektrale Auswertung des Geopotentials entlang 50 °N für Winter und Sommer. Meteor. Abh., Freie Univ. Berlin, N.F., Ser. A, Bd. **3**, Heft 3, 156 pp.

DELAND, R. J., 1973: Spectral analysis of travelling planetary scale waves: Vertical structure in middle latitudes of northern hemisphere. Tellus, **25**, 355–373.

ELIASSEN, A., and E. PALM, 1961: On the transfer of energy in stationary mountain waves. Geofis. Publ., **22**, 1–23.

FIEDLER, F., 1971: The variance spectrum of the horizontal wind velocity at 50 m above the ground. Beitr. Phys. Atmosph., **44**, 187–200.

FRAEDRICH, K., and H. BÖTTGER, 1978: A wavenumber-frequency analysis of the 500 mb geopotential at 50 °N. J. Atmos. Sci., **35**, 745–750.

FRAEDRICH, K., and H. BÖTTGER, T. DÜMMEL, 1979: Evidence of short, long and ultra-long period fluctuations and their related transports in Berlin rawinsonde data. Beitr. Phys. Atmosph., **52**, 348–361.

HAYASHI, Y., 1971: A generalized method of resolving disturbances into progressive and retrogressive waves by space Fourier and time cross-spectral analysis. J. Meteor. Soc. Japan, **49**, 125–128.

HAYASHI, Y., 1973: A method for analyzing transient waves by space-time cross spectra. J. Appl. Meteor., **12**, 404–408.

HAYASHI, Y., 1977: On the coherence between progressive and retrogressive waves and a partition of space-time power spectra into standing and travelling parts. J. Appl. Meteor., **16**, 365–373.

HAYASHI, Y., and D. G. GOLDER, 1977: Space-time spectral analysis of mid-latitude disturbances appearing in a GFDL general circulation model. J. Atmos. Sci., **34**, 237–262.

HESS, P. und H. BREZOWSKY, 1977: Katalog der Großwetterlagen Europas. Ber. Dt. Wetterd., Nr. 113.

HUNT, B. G., 1978: Atmospheric vacillation in a general circulation model I: The large-scale energy cycle. J. Atmos. Sci., **35**, 1133–1143.

KAO, S.-K., 1970: Wavenumber-frequency spectra of temperature in the free atmosphere. J. Atmos. Sci., **27**, 1000–1007.

MANABE, S., and T. B. TERPSTRA, 1974: The effects of mountains on the general circulation of the atmosphere as identified by numerical experiments. J. Atmos. Sci., **31**, 3–12.

MÜLLER, K., K. BUCHWALD and K. FRAEDRICH, 1979: Further studies on single station climatology: (i) the summer confluence of subtropic and polar front jet, (ii) the two northern cold poles. Beitr. Phys. Atmosph., **52**, 362–373.

OORT, A. H., and E. M. RASMUSSON, 1971: Atmospheric circulation statistics. NOAA Prof. Paper No. 5, U.S. Dept. of Commerce, Wash., D.C., 323 pp.

PRATT, R. W., 1976: The interpretation of space-time spectral quantities. J. Atmos. Sci., **33**, 1060–1066.

PRATT, R. W., and J. M. WALLACE, 1976: Zonal propagation characteristics of large-scale fluctuations in the mid-latitude troposphere. J. Atmos. Sci., **33**, 1184–1194.

REITER, E. R., 1969: Mean and eddy motions in the atmosphere. Mon. Wea. Rev., **97**, 200–204.

RIEHL, H., J. BADNER, J. E. HOVDE, N. E. LASEUR, L. L. MEANS, W. C. PALMER, M. J. SCHROEDER, and L. W. SNELLMAN, 1952: Forecasting in middle latitudes. Meteor. Monogr., AMS, **1**, 80 pp.

SATO, Y., 1977: Transient planetary waves in the winter stratisphere. J. Meteor. Soc. Japan, **55**, 89–105.

SCHÄFER, J., 1979: A space-time analysis of tropospheric planetary waves in the Northern Hemisphere. J. Atmos. Sci., **36**,

SPETH, P., 1974: Horizontalflüsse von sensibler und latenter Energie und von Impuls für die Atmosphäre der Nordhalbkugel. Meteorol. Rdsch., **27**, 65–90.

WILLSON, M., 1975: A wavenumber-frequency analysis of large-scale tropospheric motions in the extratropical Northern Hemisphere. J. Atmos. Sci., **32**, 478–488.

WORLD METEOROLOGICAL ORGANIZATION, 1966: Climatic change. Technical Note 79, 70 pp.